T1-Weighted Dynamic Contrast-Enhanced MR Evaluation of Different Stages of Neurocysticercosis and Its Relationship with Serum MMP-9 Expression

R.K. Gupta, R. Awasthi, R.K. Garg, N. Kumar, P.K. Gupta, A.K. Singh, P. Sahoo, V.K. Paliwal, K.N. Prasad, C.M. Pandey, and R.K.S. Rathore

ABSTRACT

BACKGROUND AND PURPOSE: Epileptogenesis in NCC is associated with perilesional inflammation and disruption in BBB. We quantified BBB in different stages of NCC by using DCE-MR imaging to look for the differences in perfusion indices and to correlate these indices with serum MMP-9 expression.

MATERIALS AND METHODS: DCE-MR imaging along with conventional MR imaging was performed in 57 single cysticercous brain lesions to quantify the k_{ep}, K^{trans}, and v_e around the lesions, which were in different stages of evolution. There were 6 lesions in the vesicular stage and 17 lesions each in the colloidal, granular-nodular, and calcified stages. Serum MMP-9 was quantified from all patients, whereas perfusion indices were quantified from all stages except for the vesicular stage.

RESULTS: We observed significant differences among the 3 stages of NCC in serum MMP-9 expression as well as DCE-derived k_{ep} values. In addition, k_{ep} showed a strongly significant positive correlation with MMP-9 expression when modeled with the individual stage of the disease as well as with all stages when pooled together. Other DCE-derived hemodynamic and pharmacokinetic parameters showed inconsistent differences with each stage of the disease. The correlation of DCE-derived parameters with serum MMP-9 expression and edema volume also showed inconsistency with the stage of the disease.

CONCLUSIONS: We conclude that k_{ep} correlates best with serum MMP-9 expression among the pharmacokinetic indices and most closely represents the degree of BBB breakdown, which is highest in the colloidal stage and lowest in the calcified stage. k_{ep} may be used as a noninvasive image biomarker of BBB breakdown in different stages of NCC.

ABBREVIATIONS: k_{ep} = rate transfer constant; K^{trans} = volume transfer coefficient; DCE= dynamic contrast-enhanced; MMP = matrix metalloproteinase; NCC = neurocysticercosis; v_e = leakage volume

NCC is a common central nervous system parasitic infection caused by the larval form of *Taenia solium*. Cysts in humans preferably lodge in the brain and spinal cord, eyes, skeletal muscle, and subcutaneous tissues.

In the brain parenchyma, the cysticercus larva passes through 4 stages.[1] In the vesicular stage, the larva appears as a cyst filled with clear fluid. This cyst has an eccentric scolex. The live cyst evokes no demonstrable inflammatory reaction. In the next stage (colloidal), inflammatory changes develop in the cyst wall and surrounding brain parenchyma because the osmotic barrier of the cyst wall breaks down. There is an intense inflammatory reaction in the surrounding brain parenchyma. The cyst wall gets progressively thickened, and hyaline degeneration and mineralization of the cyst take place. Progressive reduction in the size of the cyst, mineralization of cystic fluid, and disintegration of the scolex lead to development of a granular-nodular stage. Perilesional gliosis of brain tissue may also be seen. Ultimately, the whole cyst may be completely mineralized, resulting in a calcified stage.

Perilesional inflammation and alteration in the BBB permeability play an important role in the epileptogenesis associated with neurocysticercosis.[2-6] Many neuroinflammatory cytokines and chemokines such as intercellular adhesion molecule, interleukin-1 beta, tumor necrosis factor-alpha, and matrix metalloproteinases have been shown to be involved in the process of inflammation around the cysticercal lesion.[2,3,5,7,8] MMP-2 and MMP-9 are the 2 most widely studied MMPs, which have been shown to be critical in regulating blood-brain barrier permeability.[6,8]

Received July 8, 2012; accepted after revision August 6.

From the Departments of Radiodiagnosis (R.K. Gupta, R.A., A.K.S.), Neurology (V.K.P.), Microbiology (K.N.P.), and Biostatistics and Health Informatics (C.M.P.), Sanjay Gandhi Post Graduate Institute of Medical Sciences, Lucknow, India; Department of Neurology (R.K. Garg, N.K., P.K.G.), Chhatrapati Sahuji Maharaj Medical University, Lucknow, Uttar Pradesh, India; and Department of Mathematics and Statistics (P.S., R.K.S.R.), Indian Institute of Technology, Kanpur, Uttar Pradesh, India.

Please address correspondence and reprint requests to Rakesh K. Gupta, MD, Department of Radiodiagnosis, Sanjay Gandhi Post Graduate Institute of Medical Sciences, Raebarely Road, Lucknow, UP, India, 226014; e-mail: rakeshree1@gmail.com.

http://dx.doi.org/10.3174/ajnr.A3346

MMP-2 and MMP-9 have been demonstrated to play an important role in the development of symptoms in patients with NCC.[8,9]

It is not possible to quantify blood-brain barrier disruption by using conventional MR imaging. T1- DCE-MR imaging allows for the quantification of the physiologic indices: k_{ep}, K^{trans}, and v_e, which are directly related to the integrity of the blood-brain barrier.[6,10,11] DCE-MR imaging indices have been used to measure neoangiogenesis as well as the degree of BBB disruption in brain infection.[10-12] The pharmacokinetic indices have also been shown to correlate with MMP-9 expression.[6,10]

We hypothesized that the degree of blood-brain barrier disruption varies from the vesicular stage to the calcified stage of the cysticercal cyst, and its quantification can help us to assess the degree of inflammation around the cyst. In our study, we evaluated DCE-MR imaging in patients with different stages of the cysts to look for differences in the perfusion indices, serum MMP-9 expression, and the degree of perifocal edema. We also looked for the relationship among perfusion indices, serum MMP-9 expression, and perifocal edema, with an aim to establish these perfusion indices as noninvasive image biomarkers of quantitative BBB disruption across the different stages of NCC.

MATERIALS AND METHODS

We prospectively studied 57 patients with a single cysticercus lesion of the brain. Of these 57 patients, 51 had presented with new-onset seizures. Calcification was also reconfirmed on CT scan. We also included 6 asymptomatic patients showing the vesicular stage from the ongoing study for screening of NCC in a pig farming community. In addition, we included 10 healthy age- and sex-matched control participants to have their serum analyzed for MMP-9 estimation. The institutional ethics committee approved the study.

Imaging Characteristics of Different Stages of NCC

Cysticercous lesions were considered to be in the vesicular stage when the intensity pattern of the cyst fluid was similar to the CSF on all imaging sequences, along with the presence of a mural nodule and no surrounding edema on T2-weighted/fluid-attenuated inversion recovery images. Because the vesicular stage of these lesions does not show breakdown in the BBB and, hence, no contrast enhancement or quantifiable values of pharmacokinetic indices, we excluded 6 patients from the analysis for the purpose of BBB breakdown quantification. However, these patients as well as control participants were included for comparison of serum MMP-9 levels.

When the cystic appearance of the lesion was distinguishable by a capsule in association with perifocal edema, the cysticercus lesions were considered to be in the colloidal stage. On T2-weighted/FLAIR images, the fluid content showed a slightly higher signal than CSF. The capsule showed a slightly higher signal than the adjacent brain on T1-weighted images, a low-ring signal on T2-weighted images, and ring enhancement on postcontrast T1-weighted images. In the granular-nodular stage, the lesions were seen with a hypointense rim and a hyperintense or isointense core along with surrounding brain edema on T2-weighted images. Their rim and core were isointense or hypointense on corresponding T1-weighted images. The lesions were considered calcified when these appeared hypointense on T2-weighted images. The calcification was also confirmed on T2*-weighted angiography (SWAN) and CT images.

Data Acquisition

All study participants underwent both conventional and DCE-MR imaging on a 3T Signa HDxt MR imaging scanner (GE Healthcare, Milwaukee, Wisconsin). A 12-channel head coil was used. Conventional imaging included fast spin-echo T2-weighted images with a TE of 88 ms, a TR of 4400 ms, and number of excitations of 1; T2-weighted FLAIR with a TE of 140 ms, a TR of 9000 ms, NEX 1, and a TI of 2250 ms; T1-weighted FLAIR with a TE of 75 ms, a TR of 1600 ms, NEX of 1, and a TI of 820 ms; and postcontrast T1-FLAIR with identical parameters as that of precontrast T1-FLAIR imaging. All of these images were acquired with a field of view of 240 × 240 mm^2 and 3-mm section thickness without any intersection gap. In addition, we acquired images using the SWAN sequence (T2 star-weighted angiography; GE Healthcare) with a TE of 25 ms, a TR of 47 ms, flip angle of 15°, section thickness of 2.4 mm, acquisition matrix of 320 × 224, and an FOV of 240 × 240 mm^2 to ensure that the lesion was solitary and to demonstrate the scolex in the lesion that is pathognomonic of the disease.[13]

DCE-MR imaging was performed with a 3D spoiled gradient-recalled sequence (TR, 50 ms; TE, 21 ms; flip angle, 10°; NEX, 0.7; section thickness, 6 mm; FOV, 240 × 240 mm; matrix size, 128 × 128 mm; and number of phases, 32). At the start of the fourth acquisition, gadolinium-diethylene-triamine pentaacetic acid bis-methylamide (Omniscan, GE Healthcare) was administered intravenously through a power injector (Optistar LE; Mallinckrodt/Covidien, Hazelwood, Missouri) at 5 mL/s and a dose of 0.2 mmol/kg body weight, followed by 30 mL of saline flush. A series of 384 images during 32 time points for 12 sections were acquired (temporal resolution, 5.65 s). Before 3D spoiled gradient-recalled, T1-weighted FSE (TR, 375 ms; TE, 9.4 ms; NEX, 1; section thickness, 6 mm; FOV, 360 × 270 mm; and matrix size, 256 × 256 mm), fast double spin-echo proton-attenuation–weighted and T2-weighted (TR, 3500 ms; TE1, 25 ms; TE2, 85 ms; NEX, 1; section thickness, 6 mm; FOV, 360 × 270 mm; and matrix size, 256 × 256 mm) imaging were performed for the same section position to quantify voxelwise precontrast tissue longitudinal relaxation time (T_{10}).[11] Before MR imaging, a conventional CT scan in the axial plane from the vertex to the base of the skull was also performed to confirm the presence of calcification.

MR Imaging Data Processing and Quantitative Analysis

Voxelwise tissue longitudinal relaxation time, T_{10}, was calculated from T1, T2, and proton attenuation-weighted images obtained by FSE sequences, as described previously.[11] Quantitative analysis of the concentration-time curve was performed for calculating cerebral blood volume and cerebral blood flow. A 2-compartment pharmacokinetic model was used to calculate K^{trans}, k_{ep}, and v_e. We generated corrected CBV maps by removing the contrast agent leakage effect caused by disrupted BBBs.[14] For the calculation of perfusion indices, a k_{ep} map showing abnormal regions around the lesion were segmented, and the resulting mask was

Table 1: Mean values of DCE-MR imaging indices, serum MMP-9 expression, and edema volume for different stages of NCC

NCC Stages	rCBF	rCBV	k_{ep} (min^{-1})	K^{trans} (min^{-1})	v_e	MMP-9 (ng/mL)	Edema (cc)
Colloidal	3.53 ± 1.05	2.91 ± 1.67	1.44 ± 0.48	0.16 ± 0.11	0.11 ± 0.08	796.4 ± 273.7	18.1 ± 11.5
Granular-nodular	3.02 ± 1.36	1.94 ± 0.94	0.96 ± 0.22	0.10 ± 0.07	0.10 ± 0.07	569.3 ± 295.6	4.3 ± 1.9
Calcified	1.28 ± 0.23	1.21 ± 0.28	0.63 ± 0.36	0.02 ± 0.01	0.04 ± 0.04	214.3 ± 77.1	–
*P value	<.001	<.001	<.001	<.001	.005	<.001	<.001*

Note:—Min indicates minutes.

* Showing statistical significance on the Student *t* test. Other values are from 1-way analysis of variance.

overlaid on CBV and CBF maps to obtain CBV, CBF, K^{trans}, and v_e values. We quantified relative CBV (rCBV) and CBF (rCBF) by placing the same-size region of interest on the contralateral (healthy) side of the brain. We then quantified edema volume by calculating its visible area on all of the sections of FLAIR images. Two of the authors (R.A., P.S.), who were blinded to the patient clinical and imaging features, analyzed the data independently. There was no significant intersubject variation in the values quantified by both of these authors.

Collection of Serum Sample

We collected peripheral venous blood samples (3 mL) from all of the participants. Sera were separated, and aliquots were made and stored at −80°C until further use.

Serology Studies

Commercially available enzyme-linked immunosorbent assay (IVD Research, Carlsbad, California) and electroimmunotransfer blot were performed to detect anticysticercal antibodies in the serum. For electroimmunotransfer blot, *T solium* cyst fluid was used as the antigen.

Serum MMP-9

Commercially available enzyme-linked immunosorbent assay kits (R&D Systems, Minneapolis, Minnesota) were used to determine serum MMP-9 concentrations. All samples were measured in triplicate. According to the manufacturer's recommendations, the serum samples were diluted to a ratio of 1:100 with use of an assay buffer. The detection limit of the kit for MMP-9 is 0.31 ng/mL.

Statistical Analysis

To compare the mean values of perfusion parameters and MMP-9 for the 3 stages of NCC, we proposed 1-way analysis of variance, assuming that means of k_{ep}, K^{trans}, rCBV, and MMP-9 would be equal for all stages of NCC. The size of variation in these means is represented by their SD. The common SDs within a group for k_{ep}, K^{trans}, rCBV, and MMP-9 were assumed to be 0.7, 0.07, 1.0, and 250, respectively. The total sample size for our study for various perfusion parameters and MMP-9 on the basis of the above assumptions was computed and found to be between 33 (11 each) and 42 (14 each) patients. The requirement for k_{ep} and K^{trans} was found to be the maximal number that satisfies the assumption of other parameters. Considering that approximately 10% dropped out of the study, we found that the minimal number of patients required was 48 (16 in each group).

To compare various perfusion indices and serum MMP-9 expression in different stages of NCC, we performed 1-way analysis of variance using Bonferroni post hoc multiple comparisons. To compare edema volume in patients with stage 2 and 3 NCC, we used the Student *t* test for independent samples. In addition, the Pearson correlation coefficient was also performed to look for the association among perfusion indices, MMP-9 expression, and edema volume for each stage of NCC separately.

RESULTS

Clinical Evaluation

All patients with single cysticercal lesions had a new-onset seizure disorder. Patients with calcified lesions also presented with seizure disorders of varying duration (range, 2 weeks to 9 months).

Serology Results

A total of 39 of 57 patients tested seropositive for *T solium* on *T solium* cyst fluid-based electroimmunotransfer blot for 1 or more bands of <50kDa. However, enzyme-linked immunosorbent assay showed that 28 of 57 patients tested seropositive for anticysticercal antibody.

Lesion Distribution on Imaging and Association with Seizure Semiology

A total of 24 lesions were present in the frontal lobe, and 19 were found in the parietal lobe. In the remaining 8 patients, the parasite was located in the occipital region. Thirteen patients with frontal lobe lesions and 9 with parietal lobe lesions had contralateral focal motor seizures. Two patients with occipital lobe lesions had short-lasting visual flashes. Four patients with parietal lobe lesions had tingling sensations involving the contralateral limbs followed by secondary generalized tonic-clonic seizures. One patient with a frontal lobe lesion had a focal-onset seizure involving the contralateral lower limb followed by secondary generalization.

The patients with vesicular-stage lesions ($n = 6$) were asymptomatic and were recruited from the ongoing study for screening of NCC in a pig farming community. The lesion distribution in these patients was frontal ($n = 3$), occipital ($n = 2$), and temporal ($n = 1$).

Among 51 lesions, 17 were from the vesicular colloidal stage and 17 were from the granular-nodular and calcified stages each.

DCE-MR Imaging Metrics and Perifocal Edema Quantification

The mean values of all of the perfusion indices and edema volume are summarized in Table 1. The values of the perfusion indices decreased significantly from the colloidal to the calcified stage (Figs 1–3). Edema volume also decreased significantly from the colloidal to the granular-nodular stage. Bonferroni post hoc multiple comparisons showed (Table 2) significant differences in the colloidal and calcified stages in all perfusion indices. Significant

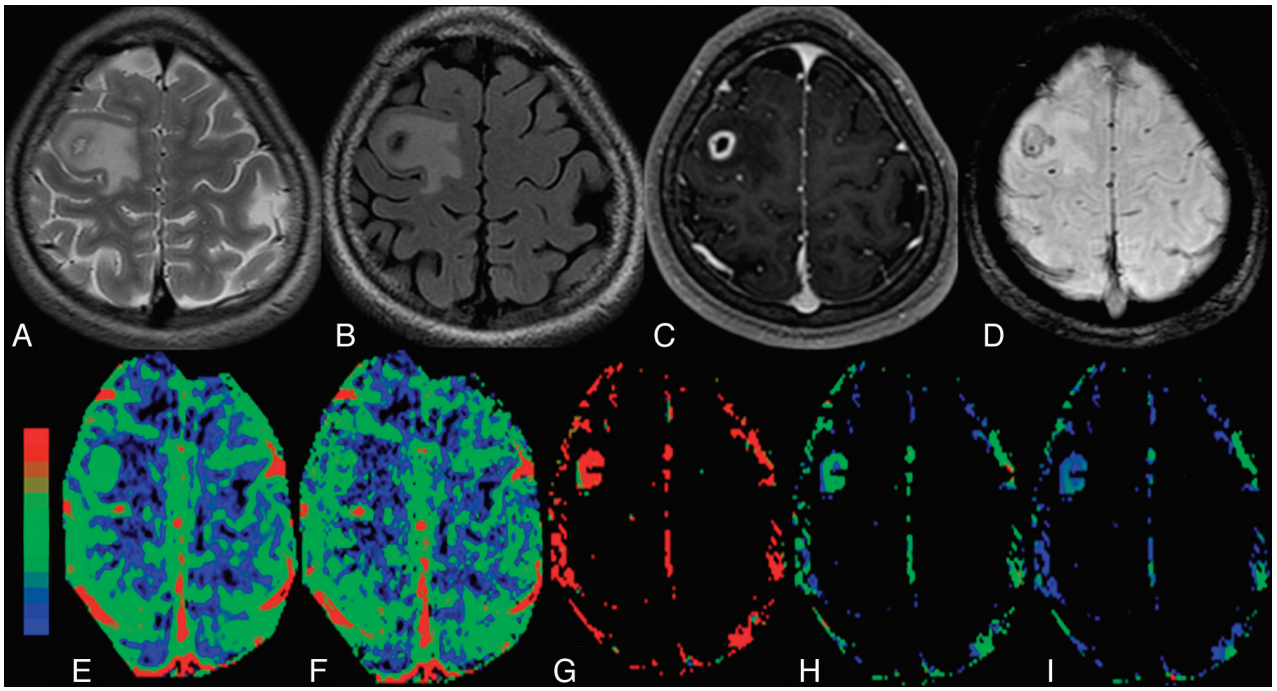

FIG 1. The colloidal stage of NCC with edema in the right frontal region in a 16-year-old girl who presented with recurrent partial seizures. *A*, The cyst appears hyperintense with a hypointense capsule on axial T2-FSE image. *B*, The cyst appears hypointense on FLAIR image with hyperintense perifocal edema. *C*, The lesion shows rim enhancement on a postcontrast T1-weighted image. *D*, Scolex is evident as an eccentric hypointense dot on SWAN image. *E–I*, On color-coded CBF [rCBF = 3.8 (*E*)], CBV [rCBV = 3.1 (*F*)], k_{ep} [k_{ep} = 1.5 minutes^{-1} (*G*)], K^{trans} [K^{trans} = 0.18 minutes^{-1} (*H*)], and v_e [v_e = 0.13 (*I*)] maps, the abnormal changes are clearly evident in and around the capsule of the lesion.

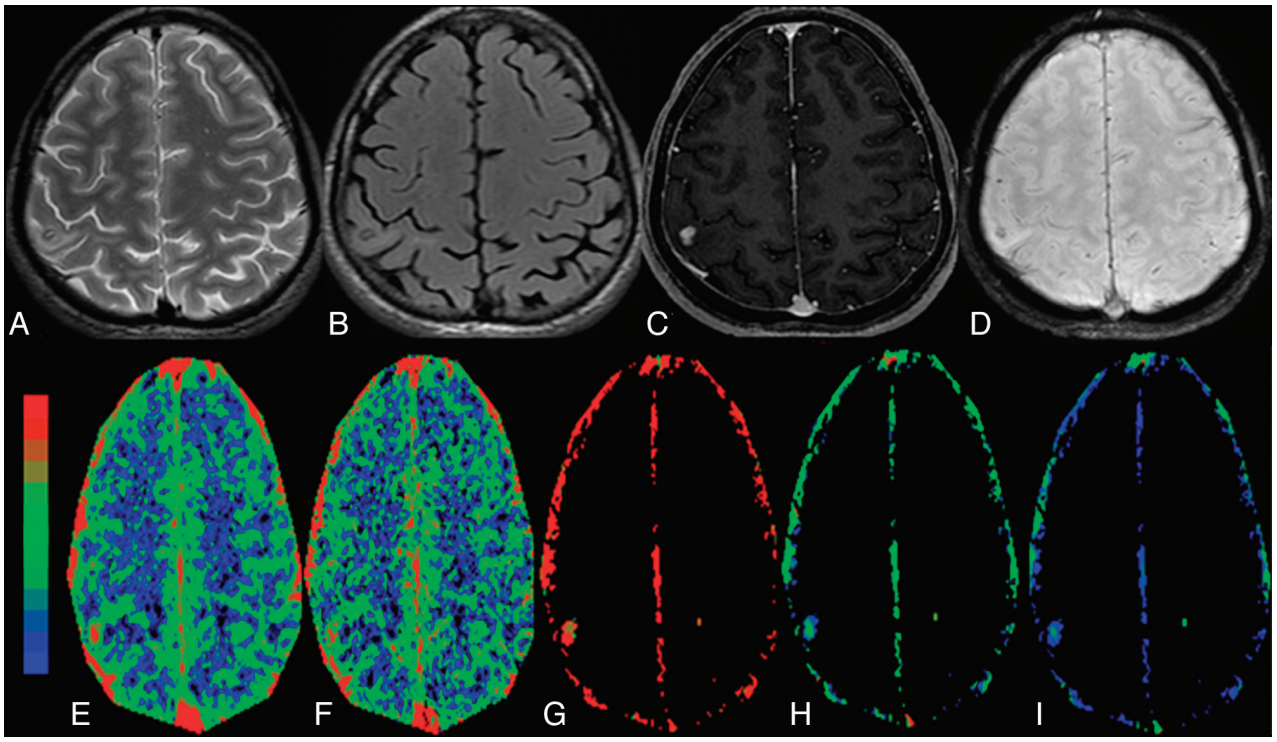

FIG 2. The granular-nodular stage of NCC with minimal edema in the right parietal region in a 32-year-old man who presented with recurrent partial seizures. The cyst appears hypointense on T2 image (*A*) and FLAIR image (*B*) with hyperintense minimal perifocal edema. *C*, The lesion shows nodular enhancement on a postcontrast T1-weighted image. *D*, On SWAN image, the lesion shows some hypointensity, which suggests minimal mineralization. On color-coded CBF [rCBF = 3.5 (*E*)], CBV [rCBV = 2.4 (*F*)], k_{ep} [k_{ep} = 1.1 minute^{-1} (*G*)], K^{trans} [K^{trans} = 0.15 minutes^{-1} (*H*)], and v_e [v_e = 0.16(*I*)] maps, the abnormal changes are clearly evident in and around the lesion.

differences were observed in the granular and calcified stages in all perfusion indices except for rCBV values. The rCBV and k_{ep} showed significant differences in the colloidal and granular-nodular stages.

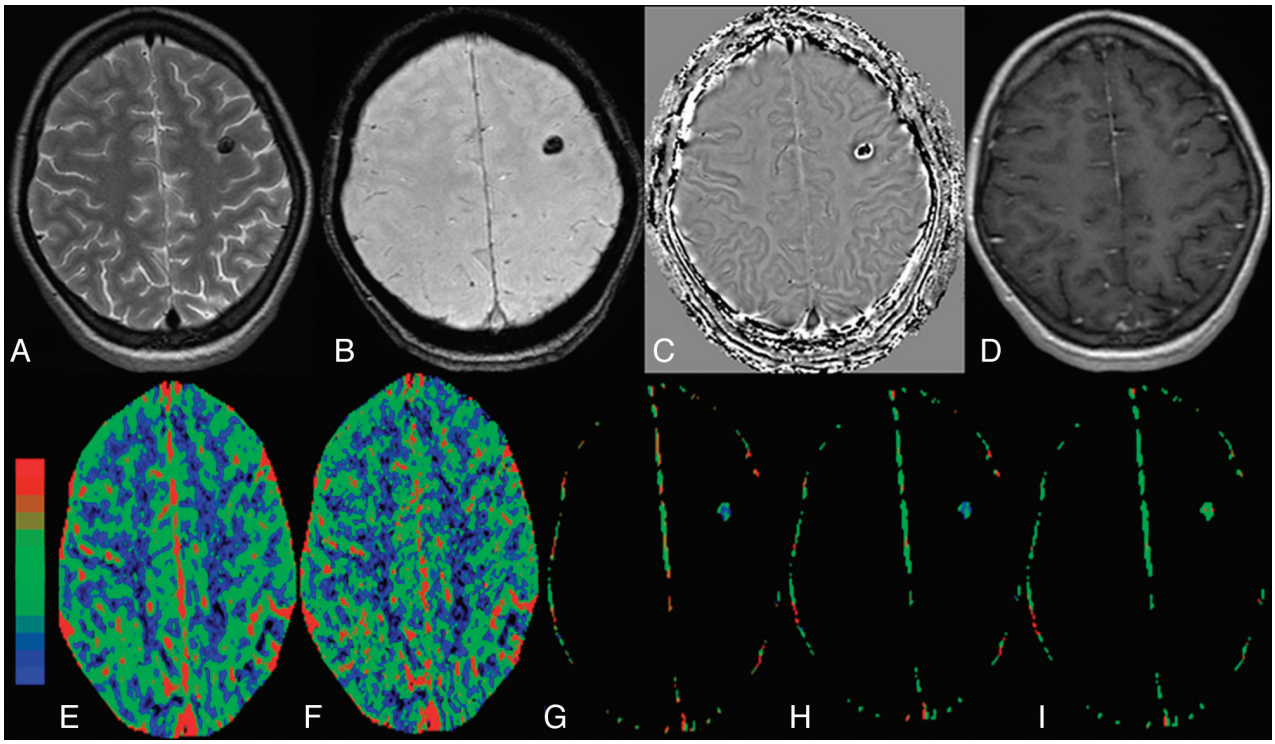

FIG 3. The calcified stage of NCC without edema in the left frontal lobe in a 34-year-old woman who presented with recurrent complex partial seizures. The lesion appears hypointense on T2 image (*A*) and SWAN image (*B*) and shows a negative phase in the center with a peripheral positive phase consistent with calcified cysticercous granuloma on a filtered phase image extracted from the SWAN imaging (*C*). Postcontrast T1-weighted image does not show any definite enhancement (*D*). On color-coded CBF [rCBF = 1.5 (*E*)], CBV [rCBV=1.3 (*F*)], k_{ep} [k_{ep} = 0.8 minutes^{-1} (*G*)], K^{trans} [K^{trans} = 0.02 minutes^{-1} (*H*)], and v_e [v_e = 0.05 (*I*)] maps, the abnormal changes are clearly evident in and around the lesion.

Serum MMP-9 Quantification

Serum MMP-9 expression was highest in the colloidal stage followed by the granular-nodular, calcified, and vesicular stages (Fig 4, Table 1). The serum MMP-9 levels were significantly lower in control, vesicular, and calcified stages compared with the colloidal and granular-nodular stages. Multiple comparisons with Bonferroni correction for serum MMP-9 expression showed significant differences in the colloidal, granular-nodular, and calcified stages (Table 2).

Relationship Between Imaging Measures and Serum MMP-9 Expression

On the Pearson correlation analysis, k_{ep} showed a strong and significant correlation with serum MMP-9 expression (Fig 5), in all of the clinically active stages of the disease individually [colloidal stage ($r = 0.62$ and $P < .01$), granular-nodular stage ($r = 0.52$ and $P = .03$), and calcified stage ($r = 0.64$ and $P < .01$)], as well as when modeled by pooling all of the stages together [($r = 0.74$ and $P < .01$)] (Fig 5). MMP-9 expression correlated significantly with rCBF ($r = 0.51$ and $P < .01$), K^{trans} ($r = 0.71$ and $P < .01$), and v_e ($r = 0.36$ and $P < .01$), as well as edema volume($r = 0.69$ and $P < .01$) when all of the data from the 3 stages were modeled together. Edema volume correlated significantly with rCBF ($r = 0.48$ and $P < .001$), *r*CBV ($r = 0.50$ and $P < .001$), k_{ep}($r = 0.57$ and $P < .001$), and K^{trans} ($r = 0.50$ and $P < .001$), as well as serum MMP-9 expression when the colloidal and granular-nodular stages of the disease were combined. However, no significant correlation of edema volume with perfusion indices was found in the colloidal and granular-nodular stages when tested for the individual stage of the disease. However, significant correlation was observed between edema and MMP-9 ($r = 0.91$; $P < .001$) in the granular-nodular stage of the disease.

DISCUSSION

In the current study, we observed significant differences among the 3 stages of NCC in serum MMP-9 expression as well as DCE-derived k_{ep} values. In addition, k_{ep} showed a strong and significant positive correlation with MMP-9 expression when modeled with the individual stage of the disease as well as when all stages were pooled together. Other DCE-derived hemodynamic and pharmacokinetic parameters showed inconsistent differences with each stage of the disease. The correlation of DCE-derived parameters with serum MMP-9 expression and edema volume also showed inconsistency with the stage of the disease.

The vesicular stage of the disease is considered as innocuous because it does not cause any perifocal inflammation, which is a prerequisite for the development of seizures.[13,15,16] It is not associated with alteration in BBB and does not show any perilesional enhancement after contrast administration.[15,16] In the current study, we did not observe any quantifiable changes in the pharmacokinetic indices k_{ep}, K^{trans}, and v_e and did not observe any peripheral enhancement on postcontrast study, reconfirming the vesicular stage of the disease. The insignificant difference in the serum MMP-9 values between patients with vesicular-stage disease and healthy control participants further confirms the integrity of the BBB.

The colloidal stage of NCC is usually associated with intense

Table 2: Multiple comparisons with use of Bonferroni test for DCE-MR imaging indices and serum MMP-9 expression

Variable	Group A vs Group B		Mean Difference	95% CI		*P* Value
	A	B		Lower Bound	Upper Bound	
rCBF	Colloidal	Calcified	2.25	1.40	3.10	<.001
	Gran Nod	Calcified	1.74	0.89	2.59	<.001
rCBV	Colloidal	Gran Nod	0.97	0.018	1.93	.045
	Colloidal	Calcified	1.67	0.74	2.65	<.001
k_{ep}	Colloidal	Gran Nod	0.49	0.17	0.80	.001
	Colloidal	Calcified	0.82	0.51	1.13	<.001
	Gran Nod	Calcified	0.33	0.02	0.65	.034
K^{trans}	Colloidal	Calcified	0.14	0.07	0.20	<.001
	Gran Nod	Calcified	0.08	0.014	0.14	.012
v_e	Colloidal	Calcified	0.07	0.017	0.13	.006
	Gran Nod	Calcified	0.06	0.001	0.11	.044
MMP-9	Colloidal	Gran Nod	227.14	25.6	428.63	.022
	Colloidal	Calcified	582.13	380.64	783.62	<.001
	Gran Nod	Calcified	354.98	153.49	556.47	<.001

Note:—Grand Nod indicates granular-nodular; CI, confidence interval.

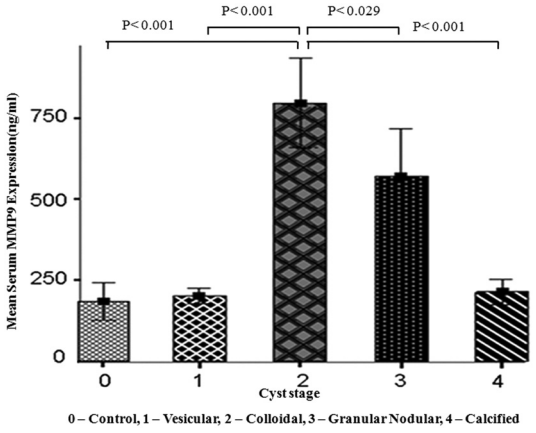

FIG 4. Bar diagram shows the mean level of serum MMP-9 expression in the control and various stages of the cyst. The colloidal stage shows a significant difference from the control, vesicular, granular-nodular, and calcified stages. The granular-nodular stage shows a significant difference from the control, vesicular, colloidal, and calcified stages. It also shows no significant difference between the control, vesicular, and calcified stages.

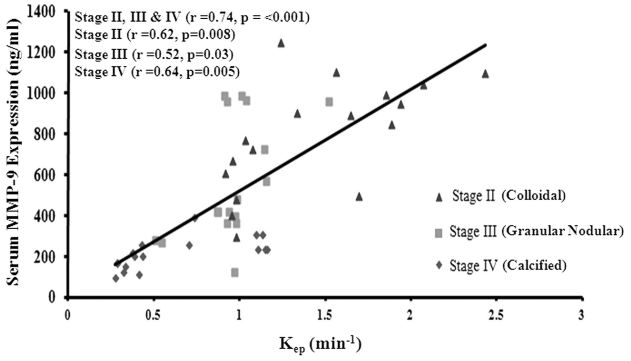

FIG 5. Scatter plots showing a significant association of serum MMP-9 levels with DCE-derived k_{ep} by use of the Pearson correlation in all 3 stages of NCC: colloidal (stage I), granular-nodular (stage II), and calcified (stage III).

perilesional inflammation and an increased breach in the BBB.[15,16] This stage is associated with the development of seizures. Postcontrast study usually shows rim enhancement. MMP-9 expression is known to get up-regulated in inflammation and is associated with breakdown in the BBB.[2,3,8,17] A link exists between the degree of inflammation and BBB breakdown. We observed the highest values of k_{ep}, K^{trans}, and v_e (Fig 1), which are the measures of BBB breakdown, in this stage of the disease. These changes are associated with maximal up-regulation of serum MMP-9 expression, which confirms that the inflammation is intense at this stage and shows the maximal breach in the BBB and correlates with it.

The granular-nodular stage of NCC shows inflammation that is less intense than the colloidal stage and is also associated with seizures.[15,16] There is a breakdown in the BBB, as suggested by the rim/disk enhancement on postcontrast study. We observed the presence of BBB breakdown as evidenced by the increase in k_{ep}, K^{trans}, and v_e (Fig 2) and increase in serum MMP-9 levels. The lower values of DCE, serum MMP-9 expression, and perifocal edema volume in this stage compared with those of the colloidal stage are in line with the observations made on histologic examination in animal studies.[3-5]

The calcified stage is considered the inactive stage of the disease and is usually labeled as the dead parasite.[13] Recently, its role in epileptogenesis and intractability of the seizures in these patients has been realized.[6,18] Indeed, some of the calcified lesions are associated with enhancement as well as with perifocal edema.[6,18] Recently, it has been shown that there may be quantifiable BBB breakdown in these lesions, even in the absence of enhancement as well as the absence of perifocal edema. Therefore, this may help to differentiate the asymptomatic from the symptomatic calcified stage of the disease.[6] In our study, though, the breakdown in the BBB was the least in calcified stage among these 3 clinically active stages of NCC that are known to cause seizures in these patients. However, these still showed enough inflammation to cause quantifiable breakdown in the BBB (Fig 3).

k_{ep} has been shown to be the best parameter for BBB breakdown in many neoplastic and infective conditions.[6,19,20] We found k_{ep} as the best parameter to measure the BBB in different stages of NCC and showed a significant difference among the 3 clinically symptomatic stages: highest in the colloidal stage and lowest in the calcified stage (Table 1). Its strong and significant positive correlation with serum MMP-9 levels in the individual stage as well as when pooled together suggests that it may be used as an image biomarker of BBB permeability in different stages of

NCC (Fig 5). It may be argued that DCE-MR imaging may be substituted by serum MMP-9 as a marker of BBB disruption, as there is a significant correlation between these 2 parameters. It is well known that serum MMP-9 levels become elevated in many non-neurologic conditions (eg, hypertension, diabetes mellitus, and atherosclerosis) and are therefore nonspecific. DCE-MR imaging measures BBB disruption specific to the lesion under investigation and, hence, adds value to both conventional MR imaging and serum MMP-9 measurements.

The degenerative stage of NCC is associated with neoangiogenesis. The neovasculature is activated secondary to the upregulation of inflammatory cytokines, including vascular endothelial growth factor. We observed the highest values of rCBV and rCBF in the colloidal stage followed by the granular-nodular and calcified stages. rCBV is considered a marker of neoangiogenesis in tumors as well as infection.[10-12] Our study reconfirms the presence of neoangiogenesis in the clinically symptomatic stages of NCC, including the calcified stage of the disease.

CONCLUSIONS

k_{ep} shows significant differences among all of the clinically active stages of NCC and is highest in the colloidal stage and lowest in the calcified stage. Correlation of k_{ep} at all of the stages of the disease with MMP-9, a marker of BBB breakdown, suggests that it may be used as a noninvasive image biomarker of BBB in the different stages of NCC. These data may form the basis of quantification of disease activity and its relationship with epileptogenesis in the future while patients are objectively assessed for therapeutic response to anticysticidal and antiepileptic therapy.

ACKNOWLEDGMENTS

R.A. acknowledges the Indian Council of Medical Research, New Delhi, India (No. 3/1/JRF/43/MPD/2007;33342) for financial support.

REFERENCES

1. Escobar A. **The pathology of neurocysticercosis.** In: Palacios E, Rodriguez-Carbajal J, Taveras J, eds. *Cysticercosis of the Central Nervous System*. Springfield, Ill: Charles C. Thomas; 1983:27–54
2. Alvarez JI, Teale JM. **Evidence of differential changes of junctional complex proteins in murine neurocysticercosis dependent upon CNS vasculature.** *Brain Res* 2007;1169:98–111
3. Alvarez JI, Teale JM. **Breakdown of the blood brain barrier and blood-cerebrospinal fluid barrier is associated with differential leukocyte migration in distinct compartments of the CNS during the course of murine NCC.** *J Neuroimmunol* 2006;173:45–55
4. Chawla S, Husain N, Kumar S, et al. **Correlative MR imaging and histopathology in porcine neurocysticercosis.** *J Magn Reson Imaging* 2004;20:208–15
5. Sikasunge CS, Johansen MV, Phiri IK, et al. **The immune response in Taenia solium neurocysticercosis in pigs is associated with astrogliosis, axonal degeneration and altered blood-brain barrier permeability.** *Vet Parasitol* 2009;160:242–50
6. Gupta RK, Awasthi R, Rathore RK, et al. **Understanding epileptogenesis in calcified neurocysticercosis with perfusion MRI.** *Neurology* 2012;28:78:618–25
7. Prasad A, Gupta RK, Pradhan S, et al. **What triggers seizures in neurocysticercosis? A MRI-based study in pig farming community from a district of North India.** *Parasitol Int* 2008;57:166–71
8. Parks WC, Wilson CL, Lopez-Boado YS. **Matrix metalloproteinases as modulators of inflammation and innate immunity.** *Nat Rev Immunol* 2004;4:617–29
9. Verma A, Prasad KN, Nyati KK, et al. **Association of MMP-2 and MMP-9 with clinical outcome of neurocysticercosis.** *Parasitology* 2011;138:1423–28
10. Haris M, Husain N, Singh A, et al. **Dynamic contrast-enhanced (DCE) derived transfer coefficient (ktrans) is a surrogate marker of matrix metalloproteinase 9 expression in brain tuberculomas.** *J Magn Reson Imaging* 2008;28:588–97
11. Singh A, Haris M, Rathore D, et al. **Quantification of physiological and hemodynamic indices using T(1) dynamic contrast enhanced MRI in intracranial mass lesions.** *J Magn Reson Imaging* 2007;26:871–80
12. Jackson A. **Imaging microvascular structure with contrast enhanced MRI.** *Br J Radiol* 2003;76:159–73
13. Del Brutto OH, Rajshekhar V, White AC Jr, et al. **Proposed diagnostic criteria for neurocysticercosis.** *Neurology* 2001;57:177–83
14. Singh A, Rathore RK, Haris M, et al. **Improved bolus arrival time and arterial input function estimation for tracer kinetic analysis in DCE-MRI.** *J Magn Reson Imaging* 2009;29:166–76
15. Garcia HH, Del Brutto OH. **Imaging findings in neurocysticercosis.** *Acta Trop* 2003;87:71–78
16. Chang KH, Lee JH, Han MH, et al. **The role of contrast-enhanced MR imaging in the diagnosis of neurocysticercosis.** *AJNR Am J Neuroradiol* 1991;12:509–12
17. Asahi M, Wang X, Mori T, et al. **Effects of matrix metalloproteinase-9 gene knock-out on the proteolysis of blood-brain barrier and white matter components after cerebral ischemia.** *J Neurosci* 2001;21:7724–32
18. Gupta RK, Kumar R, Chawla S, et al. **Demonstration of scolex within calcified cysticercus cyst: its possible role in the pathogenesis of perilesional edema.** *Epilepsia* 2002;43:1502–08
19. Awasthi R, Pandey CM, Sahoo P, et al. **Dynamic contrast-enhanced magnetic resonance imaging-derived kep as a potential biomarker of matrix metalloproteinase 9 expression in patients with glioblastoma multiforme: a pilot study.** *J Comput Assist Tomogr* 2012;36:125–30
20. Awasthi R, Rathore RK, Soni P, et al. **Discriminant analysis to classify glioma grading using dynamic contrast-enhanced MRI and immunohistochemical markers.** *Neuroradiology* 2012;54:205–13